Available online at www.sciencedirect.com
ScienceDirect
Polymer 47 (2006) 7943–7952
polymer
www.elsevier.com/locate/polymer

Kinetics of pressure-induced phase separation in polystyrene + acetone solutions at high pressures

Jian Fang, Erdogan Kiran*

Department of Chemical Engineering, Virginia Polytechnic Institute and State University, 132 Randolph Hall, Blacksburg, VA 24061, USA

Received 6 April 2006; received in revised form 29 August 2006; accepted 4 September 2006
Available online 29 September 2006

Abstract

The kinetics of pressure-induced phase separation in solutions of polystyrene ($M_w = 129{,}200$; PDI = 1.02) in acetone has been studied using time- and angle-resolved light scattering. A series of controlled pressure quench experiments with different quench depths were conducted at different polymer concentrations (4.0%, 5.0%, 8.2% and 11.4% by mass) to determine the binodal and spinodal boundaries and consequently the polymer critical concentration. The results show that the solution with a polymer concentration 11.4 wt% undergoes phase separation by spinodal decomposition mechanism for both the shallow and deep quenches as characterized by a maximum in the angular distribution of the scattered light intensity profiles. Phase separation in solutions at lower polymer concentrations (4.0, 5.0 and 8.2 wt%) proceeds by nucleation and growth mechanism for shallow quenches, but by spinodal decomposition for deeper quenches. These results have been used to map-out the metastable gap and identify the critical polymer concentration where the spinodal and binodal envelops merge.

The time scale of new phase formation and growth as (accessed) from the time evolution of scattered light intensities is observed to be relatively short. The late stage of phase separation is entered within seconds after a pressure quench is applied. For the systems undergoing spinodal decomposition, the characteristic wave number q_m corresponding to the scattered light intensity maximum I_m was analyzed by power–law scaling according to $q_m \sim t^{-\alpha}$ and $I_m \sim t^{\beta}$. The results show $\beta \approx 2\alpha$. The domain size is observed to grow from 4 μm to 10 μm within 2 s for critical quench, but about 9 s for off-critical quenches. The domain growth displays elements of self-similarity.

Keywords: Phase separation kinetics; Polymer solutions; High pressure

1. Introduction

The kinetics of phase separation in polymer systems deals with non-equilibrium relaxation processes that follow a transfer of the system from a thermodynamically stable to a thermodynamically unstable state. These transformations are usually induced by a temperature or pressure quench. The study on kinetics of phase separation of polymer mixtures or polymer solutions is important in polymer formation and processing as well as in property modifications. Information on the time scale of phase separation coupled with polymer property knowledge provides the critical criteria needed to design and control the final structure of polymer materials in particle formation or formation of microporous materials in which transient structures can be locked in.

Kinetics of phase separation in polymer systems have been mostly studied in polymer blend systems [1–7]. In a more recent investigation, Tang et al. [6] studied the temperature-induced spinodal decomposition by light scattering in blends of two copolymers, poly(styrene-*co*-methyl methacrylate) and poly(styrene-*co*-acrylonitrile), which show LCST-type phase behavior. The early stage of phase separation by spinodal decomposition was described in terms of the Cahn–Hilliard linear theory. In another study, Madbouly and Ougizawa [3] used time-resolved light scattering technique to investigate the phase separation kinetics in blends of poly(methyl methacrylate) and ploy(α-methylstyrene-*co*-acrylonitrile) which also exhibit LCST-type phase diagram, near the system's critical polymer concentration. They found that the characterization of the light scattering data for this system can also be

* Corresponding author. Tel.: +1 540 231 1375; fax: +1 540 231 5022.
E-mail address: ekiran@vt.edu (E. Kiran).

0032-3861/$ - see front matter © 2006 Published by Elsevier Ltd.
doi:10.1016/j.polymer.2006.09.015

described by the linearized Cahn–Hilliard theory during the early stage of spinodal decomposition. At the late stages of spinodal decomposition, the scaling structure function was found to be time independent, and could be described by a universal curve.

The kinetics of phase separation in "polymer + solvent" systems is of more recent but growing interest [8–13]. The phase separation in polymer solutions can be induced by changes in the temperature, the solvent (concentration or composition) or the pressure. Lal and Bansil [13] studied the kinetics of spinodal decomposition of polystyrene solutions in cyclohexane induced by a temperature jump into the unstable region. Phase separation process was monitored by time- and angle-resolved light scattering at ambient pressures. Recently, Hatanaka and Saito [11] studied the kinetics of phase separation of polycarbonate and carbon dioxide system by in situ observation of the light scattering patterns in a high pressure cell. The phase separation process was induced by increasing the temperature above LCST. These authors reported that phase separation proceeded by nucleation and growth mechanism for small temperature jumps, but by spinodal decomposition for large temperature jumps. Their study also showed that the crystallization and liquid–liquid phase separation occur simultaneously at pressures from 5 to 15 MPa and temperatures from 120 to 190 °C. Lee et al. [9] recently carried out a numerical study of temperature-induced phase separation kinetics of polymer solutions subjected to a linear spatial temperature gradient. Their results showed that anisotropic structures and morphologies can be induced by a gradient temperature jump.

In addition to temperature quench, phase separation can also be induced by exposing the solution to a nonsolvent vapor as antisolvent. An example of this is a study by Lee et al. [8] who reported the kinetics of phase separation in a polymer solution (polysulfone in *N*-methyl-2-pyrrolidinone) film induced by a nonsolvent vapor, water. The data were analyzed based on Cahn–Hilliard linear theory in the initial stages of phase separation.

In contrast to the situation with phase separation induced by temperature change or by concentration change, relatively little work has been done on the kinetics of phase separation processes induced by a pressure change. With the growing application of supercritical fluids in polymer processing, the effect of the pressure on phase separation is now attracting more interest. Compared to the thermal-induced or solvent-induced phase separation methods, the pressure-induced phase separation gives the distinct advantage in that the fast quench rates can be achieved uniformly within the system. Kojima et al. [13] have reported the early stage of spinodal decomposition during phase separation of polypropylene solution in trichlorofluoromethane induced by pressure jump using time- and angle-resolved light scattering system.

Majority of the experimental studies on pressure-induced phase separation from high pressure solution that are in the open literatures however, appears to have been generated in our own laboratory using a specially designed high pressure time- and angle-resolved light scattering system [14] suitable to carry out both shallow and deep pressure quenches at pressure up to 70 MPa and temperature up to 413 K. Kinetics of pressure-induced phase separation in poly(dimethylsiloxane) + supercritical carbon dioxide [15], polystyrene + methylcyclohexane [16] and polyethylene + *n*-pentane [17] have already been investigated using this system. Both the binodal and spinodal envelops and critical polymer concentrations in these systems have been determined by a series of pressure quenches with different quench depths in polymer solutions with different concentrations. We now report on the kinetics of phase separation in polystyrene + acetone system.

Polystyrene solutions are one of most frequently studied solutions and acetone has often been used as a model poor-solvent for polystyrene. The earliest study on the phase behavior of the solutions of polystyrene in acetone was reported by Siow et al. [19]. These solutions display both UCST and LCST phase behaviors. The effect of pressure on the phase equilibria for these systems with varying polystyrene molecular weights was later investigated by Zeman and Patterson [20] which showed that pressure increases the polymer–solvent miscibility by decreasing the UCST but increasing the LCST. Van Hook and coworkers [21–23] reported a series of investigations on the solutions of polystyrene in acetone system. The effects of pressure, temperature, polymer molecular weight, polymer concentration, and isotope effect on phase separation were investigated. A low angle (2–4° range) light scattering system was used to monitor the scattered light intensity and the transmitted light intensity as a function of time. The spinodal points (temperature or pressure) were determined by traditional extrapolation of Debye plots by assigning the spinodal point as the T or P intercept of $1/I_{sc}$ vs T or P curves. The angular variation of the scattered light intensities and its time evolution (i.e., the kinetics of phase separation) however, were not investigated by these authors.

In this paper, we report on the kinetics of phase separation in solutions of polystyrene in acetone for different concentrations in terms of the time evolution of the scattered light intensities in a time- and angle-resolved light scattering system. A series of pressure quench experiments have been carried out with different quench depths to give a complete coverage for each solution, and help to map-out the binodal and the experimentally attainable spinodal envelops.

2. Experimental section

2.1. Materials

Polystyrene of low polydispersity ($M_w = 129{,}200$, $M_w/M_n = 1.02$) was obtained from Pressure Chemical Company. The HPLC grade acetone was purchased from Emd Chemicals and was used as received.

2.2. Apparatus

Fig. 1 is a schematic diagram of the experimental system. The details of construction and operational procedures for this system have already been described in earlier publications

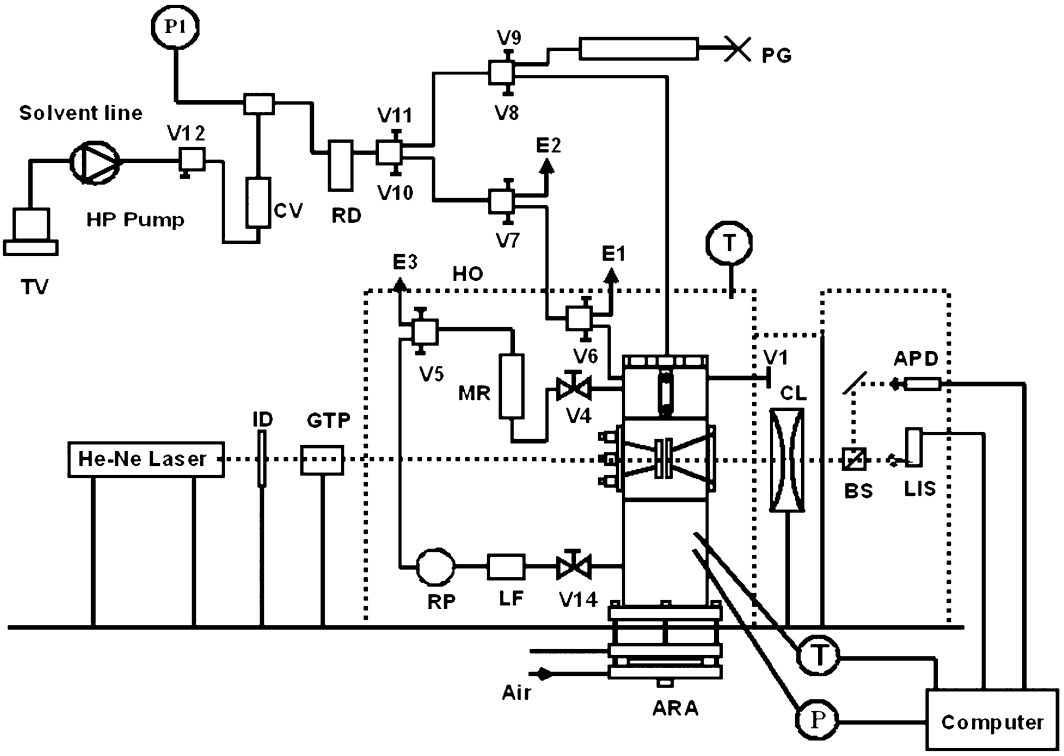

Fig. 1. Schematic of the high pressure high-temperature time- and angle-resolved light scattering systems. TV = transfer vessel; HP pump = high pressure pump; CV = check valve; RD = rupture disk; PG = pressure generator; ID = iris diaphragm; GTP = Glan–Thompson polarizer; CL = convex lens; BS = beam splitter; APD = avalanche photodiode detector; LIS = linear image sensor; HO = heated over; RP = re-circulation pump; LF = line filter; ARA = air-actuated rod assembly; MR = micro-reactor; T = thermocouple sensor; P = pressure transducer.

[14–18]. It consists of a solvent delivery line, a pressure generation line, a recirculation pump, a polymer loading and dissolution chamber, a high pressure variable volume scattering cell incorporating a movable position, and an air-actuated rod assembly and the optical light source and data collection and processing facilities. The two sapphire windows in the scattering cell are separated with a very thin stainless-steel spacer giving a path length of 250 μm. Small or intermediate pressure quenches are imposed by manipulating the pressure generator to change the position of the piston and the internal volume. For very fast or deep pressure quenches, the air-actuated expansion rod assembly is used. The optical components consist of an He–Ne laser, a Glan-Thompson polarizer and two convex lenses to collect and transfer the scattered light to a linear image sensor. The linear image sensor has 256 pixels giving a continuous angular coverage of 1.9–12.7°. A beam splitter, placed after the condensing lenses, directs the transmitted light to an Avalanche photodiode detector. During an experiment, the temperature, pressure, time, transmitted light intensity and the scattered light intensities over all angles are recorded at a rate of 3.2 ms per scan and are recorded by a dedicated computer.

2.3. Experimental procedure

The demixing pressure for a given solution is first determined as a reference point to establish the path for the pressure quench. After the desired amount of the polymer and the solvents are loaded into the system, the system is pressurized with the aid of the pressure generator at a given temperature. The high pressure recirculation pump is activated to homogenize the contents in the system and achieve dissolution. The homogeneous conditions are verified by visual observations through the sapphire windows. The demixing pressure is determined by decreasing the system pressure until the two-phase region is entered. When the system crosses the phase boundary, the pressure corresponding to the departure from the base value of the transmitted light, or the inverse scattered light is identified as the demixing pressure. These are illustrated in Fig. 2 for a 7.4 wt% solution, in which pressure was reduced from about 52 to 40 MPa over about 40 s. With the initiation of the pressure reduction, system shows a small but observable temperature reduction which leads to small fluctuation in the transmitted light intensities. The effect is smaller with the scattered light intensities. The scattered light intensities shown in this plot are the average values over the full angle range. As shown in the figure, the $1/I_s$ is more stable and thus is preferred in assigning the demixing (binodal) pressure. After the quench is completed, as the system tries to reheat to the initial temperature, a pressure rise is noted from about 39 to 40 MPa.

Once the demixing pressures are determined, the solution is rehomogenized at a pressure about 2 MPa above the demixing pressure. Then, at a given temperature, the pressure is carefully brought to about 0.1 MPa above the demixing pressure. The system is then subjected to a controlled shallow or deeper pressure quench. This is demonstrated in Fig. 3 for a solution

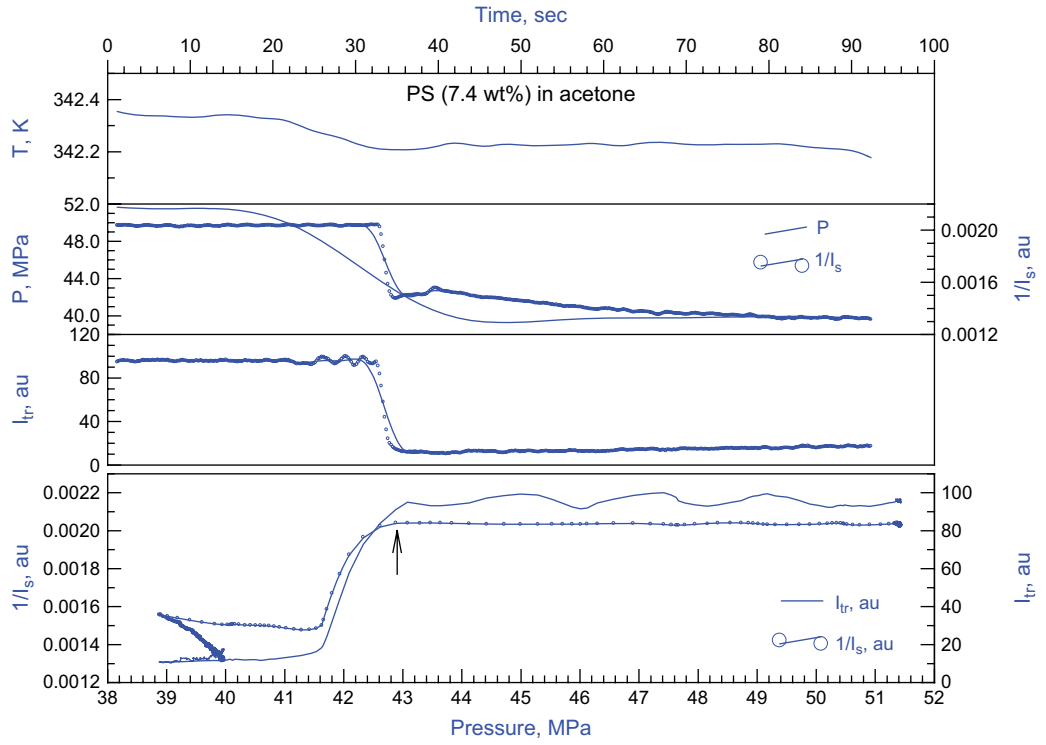

Fig. 2. Variation of temperature (T), pressure (P), transmitted light intensity (I_{tr}) (in arbitrary units) and inverse average scattered light intensity $(1/I_s)$ with time during a pressure reduction. The demixing pressure is determined from the variation of the inverse scattered light intensity with temperature (lower curve in the figure) as the point of departure from the base line intensity as indicated by arrow. The figure represents phase separation in 7.4 wt% solution of polystyrene in acetone and at $T = 342$ K.

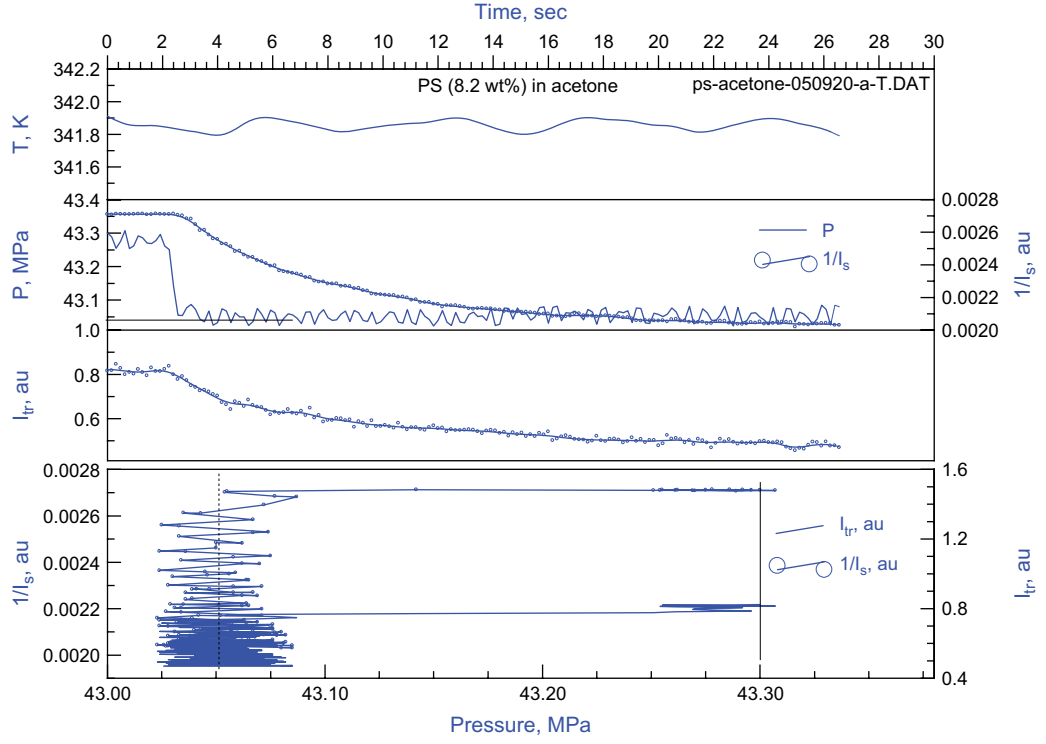

Fig. 3. Variation of temperature (T), pressure (P), transmitted light intensity (I_{tr}), and inverse averaged scattered light intensity $(1/I_s)$ with time during a 0.25 MPa pressure reduction in 8.2 wt% solution of polystyrene in acetone.

of 8.2 wt% polystyrene in acetone undergoing a pressure quench depth of 0.25 MPa. The total time for completion of the quench is around 0.5 s corresponding to a quench rate of 0.5 MPa/s. In the present study, the majority of the quenches was controlled by adjusting the pressure generator. The pressure quench depths were varied from 0.1 to 3 MPa.

The time evolution and the angular variation of the scattered light intensities show different trends if the solution is undergoing phase separation by nucleation and growth or by spinodal decomposition. Systems undergoing phase separation by spinodal decomposition show a maximum in the angular variation of the scattering light intensities, while for systems undergoing phase separation by nucleation growth, the angular distribution of scattered light intensities does not display such as a maximum and decreases with angle. The experiments were carried out at each concentration for different quench depths to determine the crossover pressure from one type of phase separation mechanism to another.

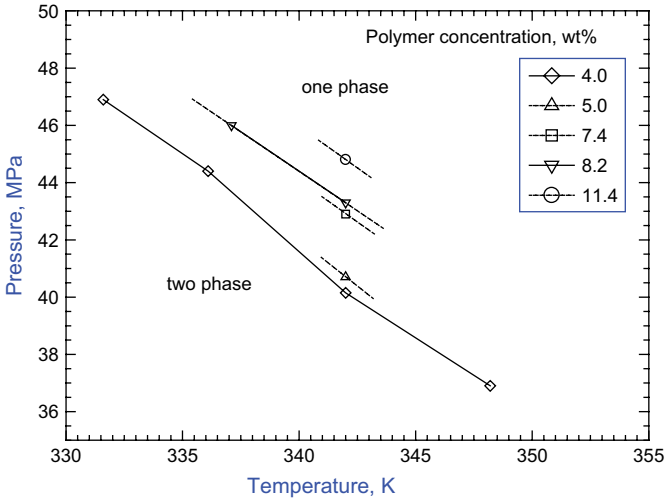

Fig. 4. Pressure–temperature phase diagram showing the experimentally determined demixing boundaries for 4.0 and 8.2% solutions of PS (129.2 K) + acetone. The demixing pressure data at 342 K for 5.0, 7.4 and 11.4% solutions are also shown in the figure. The system shows a USCT type phase behavior in the experimental temperature range.

3. Results and discussion

The demixing pressures are first determined as the reference points for the quench experiments. Fig. 4 shows demixing curves for PS + acetone system at different concentrations in pressure–temperature (P–T) diagram. For the solution at 4.0 wt%, the experimental temperature range was 331 to 348 K; and for the solution at 8.2 wt%, the temperature range was 337–342 K. At 342 K, the demixing pressures were determined for three other solutions with concentrations of 5.0, 7.4, and 11.4% and are included in Fig. 3. In the figure, the region above each line is one-phase region. The negative slopes of these lines indicate that the systems display upper critical solution temperature (UCST) type phase behavior in the experiment range.

As indicated earlier, the phase behavior of polystyrene in acetone solutions has been investigated also by other groups [20,21]. The present results even though obtained with a higher molecular weight polystyrene sample are in a good agreement with these earlier reports. Zeman and Patterson [20] reported the cloud point curves for several polystyrene samples with different molecular weights [from 20,400 to 97,200] which include both UCST and LCST branches in a T, P diagram. Our present results with 11.4 wt% polystyrene (with a molecular weight of 129,200) solution show phase separation at a temperature of 342 K (69 °C) and pressure of 42.80 MPa (428 bar), which lies above the cloud point curve for the 14.6 wt% solution for a lower molecular weight ($M = 97{,}200$) sample reported in the earlier study. The results are consistent, with miscibility decreasing with increasing polymer molecular weight.

Pressure quench experiments with different quench depths were then conducted at polymer concentrations of 4.0, 5.0, 8.2 and 11.4 wt% at 342 K.

Fig. 5 shows the time evolution of the scattered light intensities as a function of the wave vector q (which is equal to $(4\pi/\lambda)\sin(\theta/2)$) for a quench depth of $\Delta P = 0.70$ MPa at 342.1 K for 4.0 wt% solution. Here, λ is wave

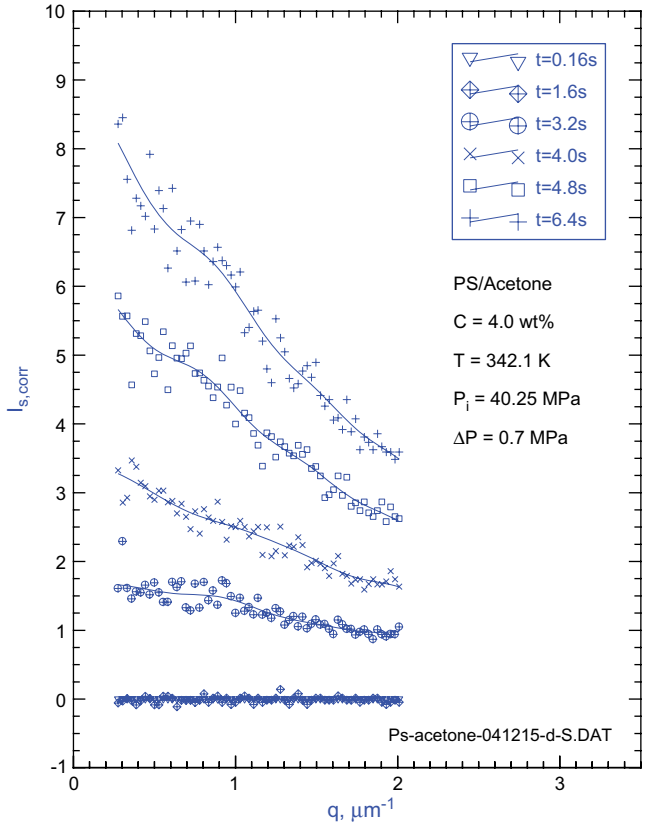

Fig. 5. Scattered light intensity profiles as a function of wave number (scattering angle) and time for a pressure quench in 4.0% by mass polystyrene solution in acetone at 342 K. The quench depth is $\Delta P = 0.70$ MPa.

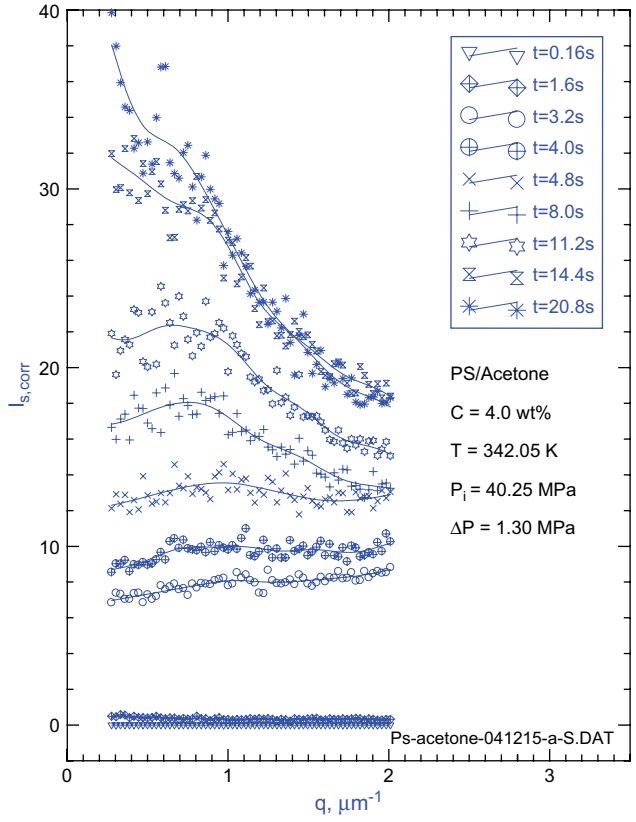

Fig. 6. Scattered light intensity profiles as a function of wave number (scattering angle) and time for a pressure quench in 4.0% by mass polystyrene solution in acetone at 342 K. The quench depth is $\Delta P = 1.30$ MPa.

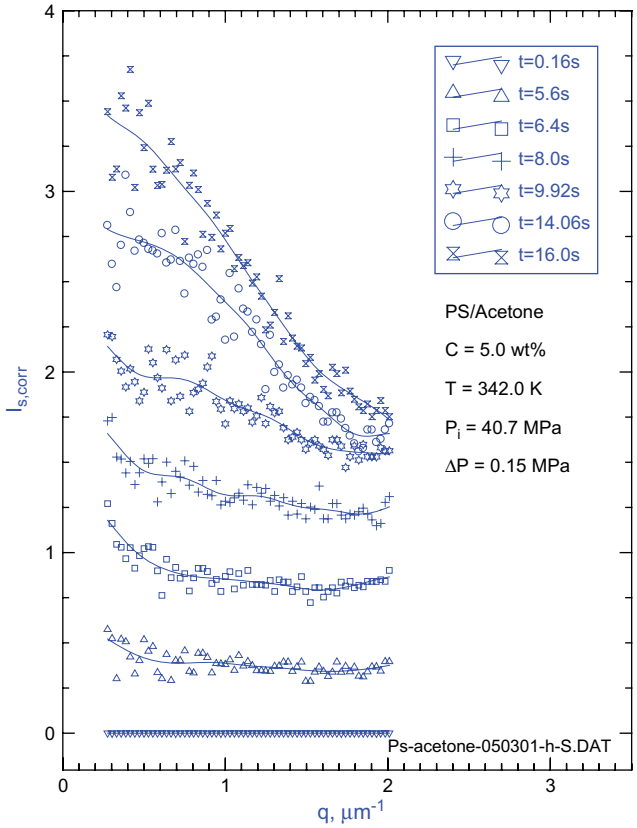

Fig. 7. Scattered light intensity profiles as a function of wave number (scattering angle) and time for a pressure quench in 5.0% by mass polystyrene solution in acetone at 342 K. The quench depth is $\Delta P = 0.15$ MPa.

length of the laser light [$\lambda = 632.8$ nm], and θ is the scattering angle. The scattered light intensities increase with time, but show continual decrease with increasing scattering angles. This is typical of systems undergoing phase separation by nucleation and growth. Fig. 6 shows the results when the solution was subjected to a greater quench depth of 1.30 MPa. Here, a maximum in angular distribution of the scattered light intensity profile was observed to develop shortly after the quench. The formation of scattering maximum is typical of systems undergoing phase separation by spinodal decomposition. The position of the maximum is noted to move to lower q values with increasing time. The metastable gap that is the quench depth to enter the spinodal decomposition for this solution was observed to be over 0.6 MPa.

Fig. 7 shows the scattered light intensity profiles during phase separation for 5.0 wt% solution when subjected to 0.15 MPa quench at 342 K. Fig. 8 shows the results for a deeper quench (0.4 MPa) of this system. Formation of the spinodal ring is distinctly observed after about 4.0 s, which is shortly after the completion of the pressure quench. Figs. 9 and 10 show the evolution of the scattered light intensity in 8.2% solutions. The quench depths are $\Delta P = 0.10$ and 0.25 MPa, respectively. The results show the crossover from nucleation and growth to spinodal decomposition in deeper quenches.

Figs. 11 and 12 show the scattered light intensity profile for two different quench depths $\Delta P = 0.10$ and 0.35 MPa, respectively, for a solution at a higher concentration of 11.4 wt%. With this solution, the maximum in the scattered light intensity profile is observed to develop shortly after the quench regardless of the quench depth. This observation suggests that the critical polymer concentration must be at or very close to 11.4 wt%.

Table 1 summarizes the results of binodal and spinodal pressures (all generated from the quench experiments). Fig. 13 shows these and the regions where nucleation and growth were observed in a pressure–concentration phase diagram (P–X). The figure clearly demonstrates the narrowing of the metastable gap in going from 4.0 to 11.4 wt% solutions. The binodal and spinodal curves merge at critical polymer concentration.

In an earlier study, the temperature-induced spinodal decomposition in polystyrene + acetone solution had been explored by Szydlowski et al. [21]. The spinodal decomposition temperatures of polystyrene (the molecular weight up to 11,500) solutions in acetone solutions were determined from extrapolation of the light scattering data at a fixed angle using Debye plots. Even though in that study, a plausible use of the apparatus to determine the spinodal decomposition pressures in a pressure-induced phase separation is also stated, no detailed data on spinodal decomposition pressures were reported.

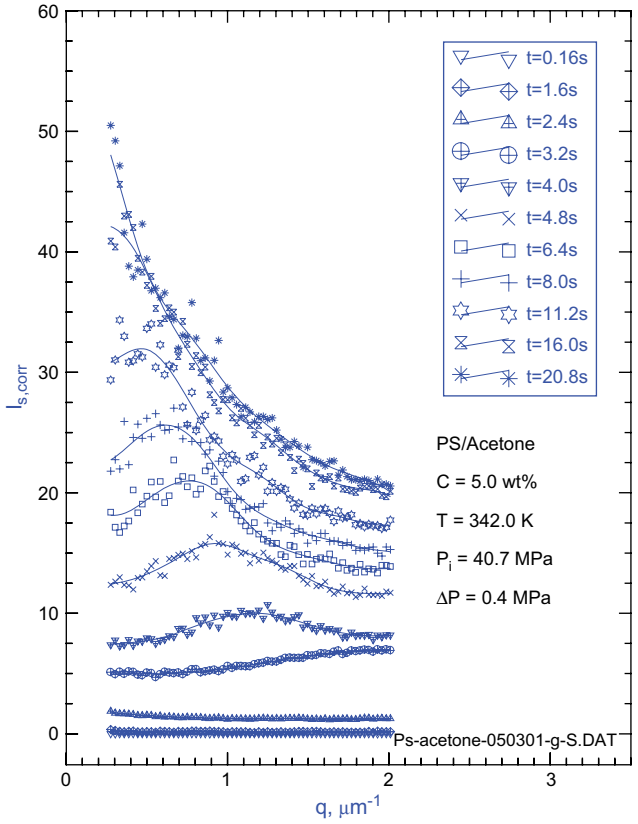

Fig. 8. Scattered light intensity profiles as a function of wave number (scattering angle) and time for a pressure quench in 5.0% by mass polystyrene solution in acetone at 342 K. The quench depth is $\Delta P = 0.50$ MPa.

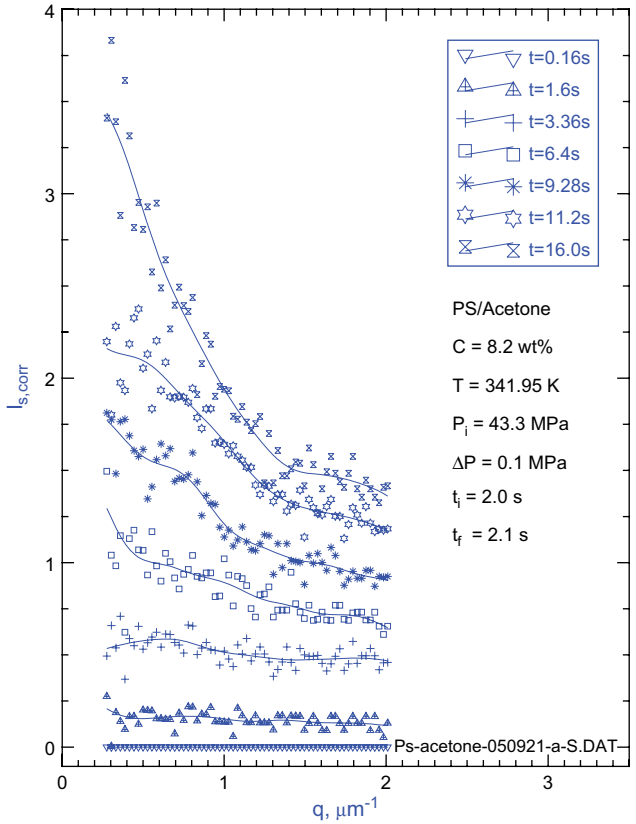

Fig. 9. Scattered light intensity profiles as a function of wave number (scattering angle) and time for a pressure quench in 8.2% by mass polystyrene solution in acetone at 342 K. The quench depth is $\Delta P = 0.10$ MPa.

4. Further analysis of the time evolution of the scattered light intensity and the characteristic domain size

For the early stage of spinodal decomposition, Cahn–Hilliard theory [24] predicts that the scattered light intensity should increase with time exponentially according to

$$I(q,t) = I(q,0)\exp(2R(q)t) \tag{1}$$

Here q is again the wave number of growing fluctuations and $R(q)$ is the rate of growth of concentration fluctuations given by

$$q = \frac{4\pi}{\lambda}\sin(\theta/2) \tag{2}$$

$$R(q) = D_{\mathrm{app}}q^2\left[1 - \frac{q^2}{2q_{\mathrm{m}}^2}\right] \tag{3}$$

where D_{app} is the apparent diffusivity and q_{m} is the wave number corresponding to maximum growth rate of fluctuations. The apparent diffusivity can be calculated from plots of $R(q)/q^2$ as the limiting value of $R(q)/q^2$ as q approaches to 0, that is

$$D_{\mathrm{app}} = \lim_{q\to 0}\{R(q)/q^2\} \tag{4}$$

Linearized Cahn–Hilliard theory is strictly applicable over the time interval in which the location of the maximum in the scattered light intensity does not change with time. However, as shown in Figs. 8–11, in the solutions undergoing spinodal decomposition, the spinodal ring is not stationary and the wave number q_{m} corresponding to the maximum in the scattered light intensity I_{m} moves to lower q values with time. Thus the observation times in the present experiments, even though very short compared to observation times encountered in experiments with polymer blends or alloys, are not short enough to capture the new phase formation and evolution in the very early stages of the spinodal decomposition.

The intermediate and late stages of spinodal decomposition are often described in terms of power–law relationships [17,25] of the type

$$I_{\mathrm{m}}(t) \approx t^{\beta} \tag{5}$$

$$q_{\mathrm{m}}(t) \approx t^{-\alpha} \tag{6}$$

These relationships provide a scaling description in terms of the exponents β and α of the time evolution of the scattered light intensity maximum I_{m} and the corresponding wave number q_{m}.

Fig. 14(a) shows the variation of $\log(q_{\mathrm{m}})$ and $\log(I_{\mathrm{m}})$ with $\log(t)$ for 8.2 wt% solution subjected to 0.25 MPa

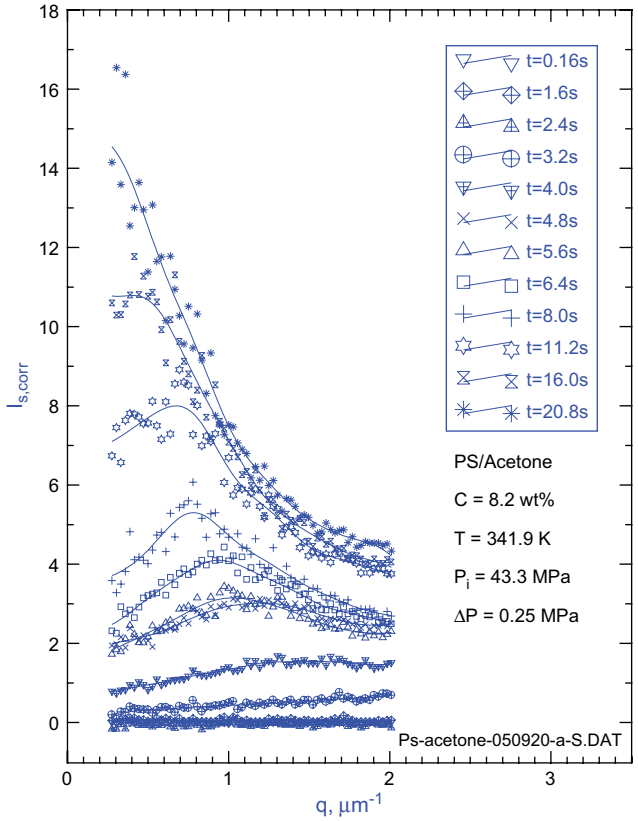

Fig. 10. Scattered light intensity profiles as a function of wave number (scattering angle) and time for a pressure quench in 8.2% by mass polystyrene solution in acetone at 341.9 K. The quench depth is $\Delta P = 0.25$ MPa.

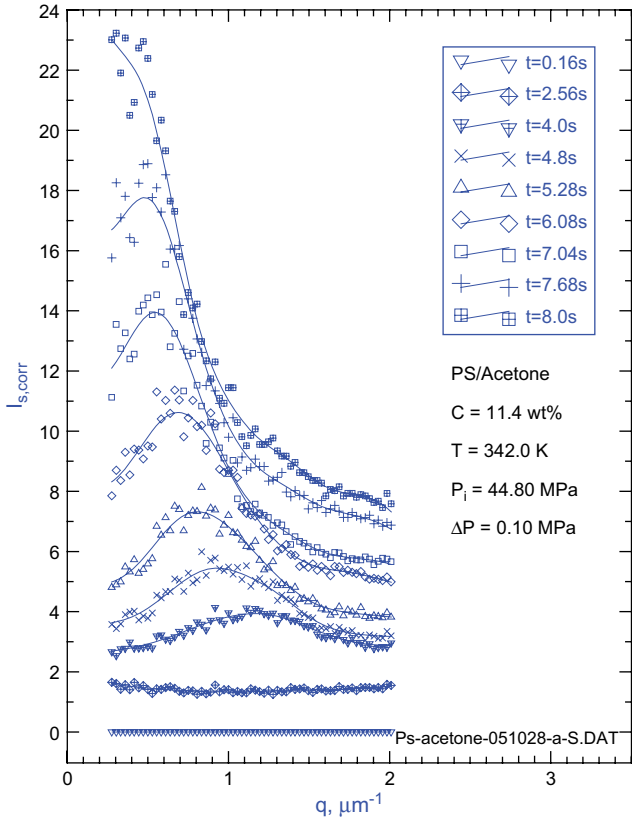

Fig. 11. Scattered light intensity profiles as a function of wave number (scattering angle) and time for a pressure quench in 11.4% by mass polystyrene solution in acetone at 342.0 K. The quench depth is $\Delta P = 0.10$ MPa.

quench at 341.9 K corresponding to the data shown in Fig. 10. Analysis of Fig. 14(a) shows that the growth exponent α for q_m is 0.74 and β for I_m is 1.46 which suggests $\beta \approx 2\alpha$. Such dependence has also been observed for polystyrene + cyclohexane [13] system undergoing temperature-induced phase separation and for polystyrene + methylcyclohexane [16], polydimethylsiloxane + carbon dioxide [15] and polyethylene + *n*-pentane [17] systems undergoing pressure-induced phase separation. Fig. 14(b) shows the results for 11.4 wt% solution subjected to 0.10 MPa quench at 342 K. The growth exponent α is 1.39 and β is 2.18 for this quench, giving a relationship of $\beta \approx 1.6\alpha$. As theoretically predicted by Kawasaki and Ohta [28] and Furukawa [27], the simple scaling relation is not valid over the large time region of phase separation and the exponent α itself becomes a time dependent parameter. The value of α increases with progress of phase separation. Comparing with the two values of α determined from previous data, even with a shallow pressure quench, the polymer solution at the critical concentration or near to critical concentration undergoes a faster phase separation than that at off-critical concentrations. At the same time scale, a late stage of phase separation may be captured for the critical quench.

The maximum value of the wave number q_m is related to the domain size scale, which is expressed as [26]

$$L = 2\pi/q_m \tag{7}$$

The domain size continuously increases during this time interval of the phase separation process. Fig. 15 shows a plot of the evolution of the characteristic domain size with time in the two solutions shown in Fig. 14. The domain sizes reach about 5 μm in 1 s after quench is finished and approaches about 15 μm within 5 s for the 11.4% solution with 0.10 MPa quench, while for 8.2% solution, the domain size reaches 4 μm in 1 s and approaches about 18 μm in 14 s. Comparison of the two systems suggest that the 11.4% solution with 0.10 MPa quench shows a faster growth rate than the 8.2% solution with 0.25 MPa quench. It is worth to mention that even though the stationary q_m region has not been experimentally captured, the data suggest that a domain size of 5 μm is reached in the early stage of phase separation.

For systems that display dynamic similarity, Furukawa [27] has developed scaling functions given by

$$F(x) = 4x^2/(3 + x^8) \text{ (critical quench)} \tag{8}$$

$$F(x) = 3x^2/(2 + x^6) \text{ (off-critical quench)} \tag{9}$$

Where $F(x)$ is the structure factor expressed as $F(x) \approx I(x)/I_m(t)$ and $x = q/q_m(t)$. In such systems, the plot of $F(x)$ vs x should collapse to a single curve for all

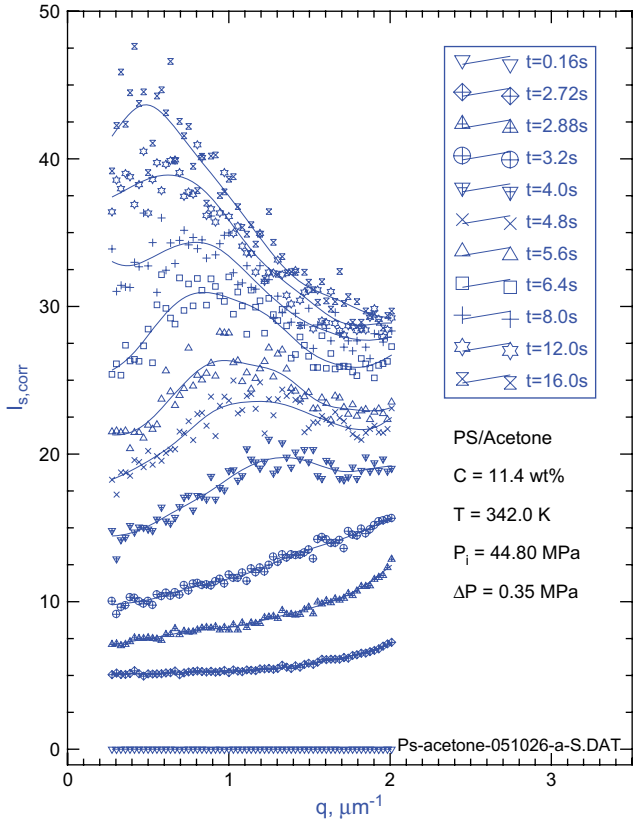

Fig. 12. Scattered light intensity profiles as a function of wave number (scattering angle) and time for a pressure quench in 11.4% by mass polystyrene solution in acetone at 342.0 K. The quench depth is $\Delta P = 0.35$ MPa.

Table 1
Binodal and spinodal points of solutions of polystyrene ($M_w = 129{,}200$) in acetone ($T = 342$ K)

Polymer concentration (wt%)	Demixing pressure (MPa)	Spinodal pressure (MPa)
4.0	40.15	39.20
5.0	40.70	40.40
8.2	43.30	43.13
11.4	44.80	44.75

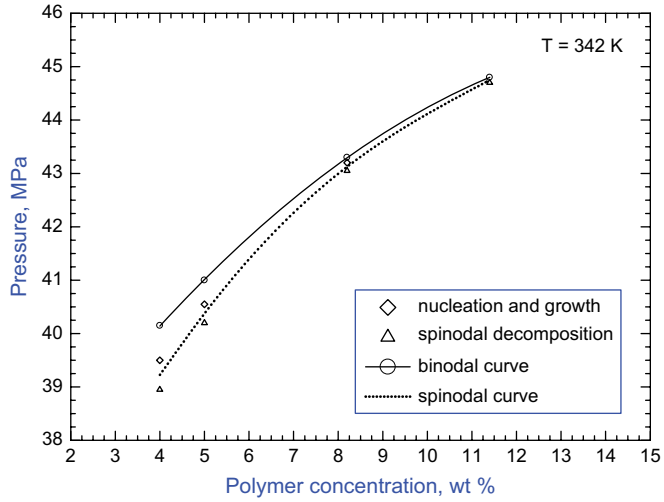

Fig. 13. Pressure–composition phase diagram and the experimentally determined spinodal and binodal curves for PS (129.2 K) + acetone system at 342 K.

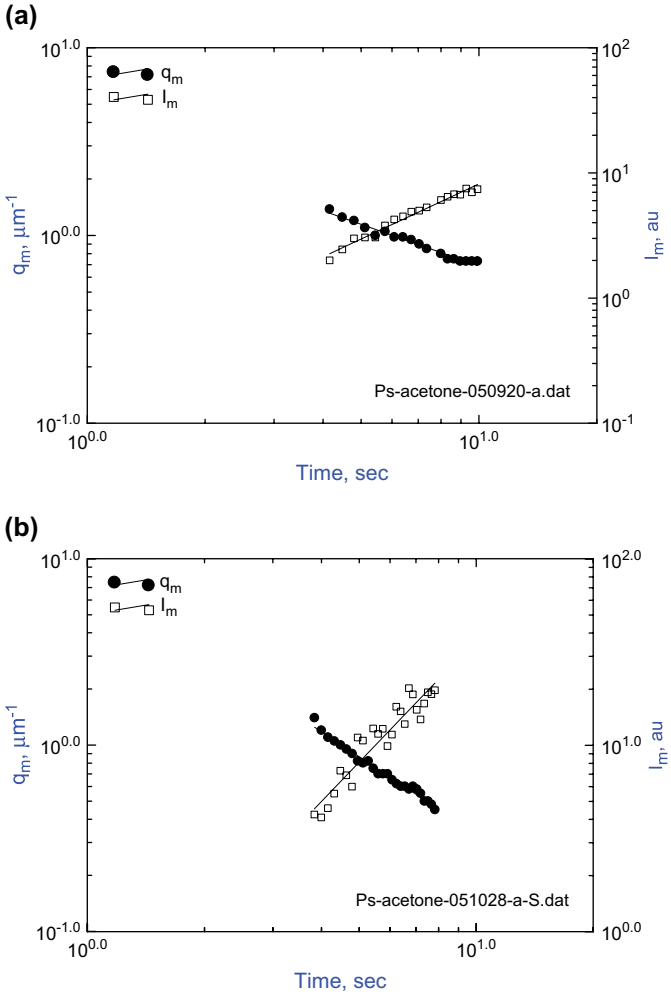

Fig. 14. Power–law dependence of q_m and I_m on time. (a) The data correspond to 8.2 wt% solution subjected to 0.25 MPa quench as shown in Fig. 10. (b) The data correspond to 11.4 wt% solution subjected to 0.1 MPa quench as shown in Fig. 11.

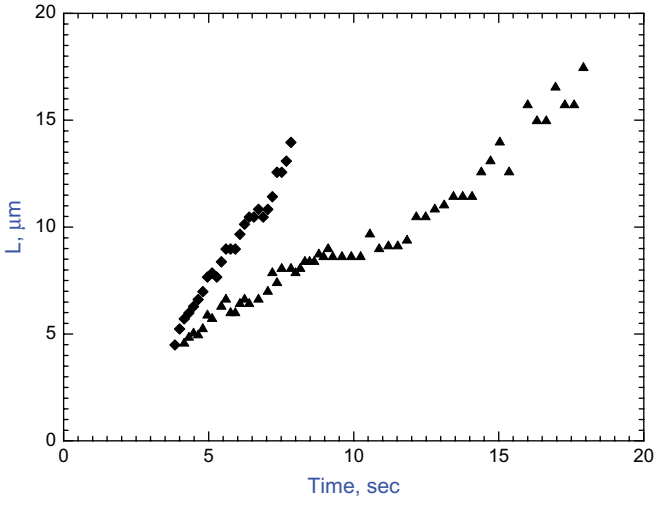

Fig. 15. Evolution of the domain size with time: the triangle data correspond to 8.2 wt% solution subjected to 0.25 MPa quench as shown in Fig. 10 and the diamond data correspond to 11.4 wt% solution subjected to 0.10 MPa quench as shown in Fig. 11.

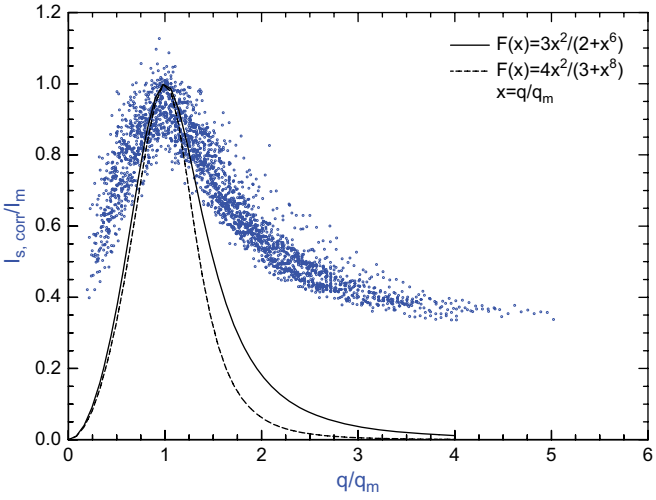

Fig. 16. Test of dynamic scaling hypothesis for the reduced structure factor. The data correspond to 8.2 wt% solution subjected to 0.25 MPa quench as shown in Fig. 10. The different time data scale collapse toward a master curve. The solid and dotted curves are the predications from the Furukawa universal scaling functions for off-critical and critical quenches, respectively.

times. Fig. 16 shows such a plot for the 8.2 wt% solution at 342 K for a 0.25 MPa pressure quench, corresponding to the time evolution data shown in Fig. 10. As shown in the figure, the reduced data points indeed collapse to a single curve, which suggests self-similarity. However, the experimental data do not obey the theoretical Furukawa scaling functions. The theoretical curves are also included in Fig. 16 for comparison purpose. The experimental data deviate more from the theoretical Furukawa scaling expectations as q moves away from q_m.

5. Conclusions

The present results show that the mechanisms of pressure-induced phase separation in polystyrene + acetone solutions can clearly be differentiated by using time- and angle-resolved light scattering systems. For critical or near critical quenches, the spinodal regime is observed for both shallow and deep quenches. The critical concentration is determined to be 11.4%. For off-critical quenches, the mechanism of phase separation is found to be varying with quench depths, and the nucleation and growth regimes are observed for shallow quenches and the spinodal regimes are observed for deep quenches. The metastable gap becomes larger when the polymer concentrations are further apart from the critical polymer concentration. The early stage of spinodal decomposition is relatively short. The kinetics of spinodal decomposition in intermediate and late stage is well described by the power–law scaling models. The domain growth displays features of self similarity.

References

[1] Binder K, Fratzl P. In: Kostorz G, editor. Phase transformations in materials. Weinheim: Wiley-VCH; 2001. p. 409.
[2] Rappl TJ, Balsara NP. J Chem Phys 2005;122:214903.
[3] Madbouly SA, Ougizawa T. Macromol Chem Phys 2004;205:979.
[4] Henderson IC, Clarke N. Macromolecules 2004;37:1952.
[5] Aksimentiev A, Holyst R, Moorthi K. Macromol Theory Simul 2000; 9:661.
[6] Tang P, Arrighi V, Higgins JS, Li GX. Polym Int 2004;53:1686.
[7] Hashimoto T, Kumaki J, Kawai H. Macromolecules 1983;16:641.
[8] Lee HJ, Jung B, Kang YS, Lee H. J Membr Sci 2004;245:103.
[9] Lee KD, Chan PK, Feng XS. Chem Eng Sci 2004;59:1491.
[10] Kuwahara N, Tachikawa M, Hamano K, Kenmochi Y. Phys Rev A 1982; 35:3449.
[11] Hatanaka M, Saito H. Macromolecules 2004;37:7358.
[12] Kojima J, Takenaka M, Kakayama Y, Hashimoto T. Macromolecules 1999;32:1809.
[13] Lal J, Bansil R. Macromolecules 1991;24:290.
[14] Xiong Y, Kiran E. Rev Sci Instrum 1998;69:1463.
[15] Liu K, Kiran E. J Supercrit Fluid 1999;16:59.
[16] Xiong Y, Kiran E. Polymer 2000;41:3759.
[17] Liu K, Kiran E. Macromolecules 2001;34:3060.
[18] Zhuang WH, Kiran E. Polymer 1998;39:2903.
[19] Siow KS, Delmas G, Patterson D. Macromolecules 1972;5:29.
[20] Zeman L, Patterson D. J Phys Chem 1972;76:1214.
[21] Szydlowski J, Rebelo LP, Van Hook WA. Rev Sci Instrum 1992;63:1717.
[22] Szydlowski J, Van Hook WA. Macromolecules 1991;24:4883.
[23] Luszczyk M, Rebelo LPN, Van Hook WA. Macromolecules 1995;28:745.
[24] Cahn JW. J Chem Phys 1959;30:1121.
[25] Takenaka M, Kojima J, Nakayama Y, Hashimoto T. Polymer 2005; 46:10782.
[26] Hashimoto T. In: Imanishi Y, editor. Progress in pacific polymer science, vol. 2. Berlin: Springer; 1992. p. 175.
[27] Furukawa H. Adv Phys 1985;34:703.
[28] Kawasaki K, Ohta T. Prog Theor Phys 1978;59:362.